Fabrication of MIP-201 Membrane with Excellent Stability for High-Efficiency Uranium Separation from Seawater

Yue Zhang, Jiaxin Liu, Shishi Du, Tingting Wang, Meixi Yan, Sixing Chen, Sujing Wang, Xin Zheng, Jing Ma, Shin-ichiro Noro, Yi Liu

PII: S0376-7388(25)01234-7

DOI: https://doi.org/10.1016/j.memsci.2025.124921

Reference: MEMSCI 124921

To appear in: Journal of Membrane Science

Received Date: 18 July 2025

Revised Date: 25 October 2025 Accepted Date: 9 November 2025

Please cite this article as: Y. Zhang, J. Liu, S. Du, T. Wang, M. Yan, S. Chen, S. Wang, X. Zheng, J. Ma, S.-i. Noro, Y. Liu, Fabrication of MIP-201 Membrane with Excellent Stability for High-Efficiency Uranium Separation from Seawater, *Journal of Membrane Science*, https://doi.org/10.1016/j.memsci.2025.124921.

This is a PDF of an article that has undergone enhancements after acceptance, such as the addition of a cover page and metadata, and formatting for readability. This version will undergo additional copyediting, typesetting and review before it is published in its final form. As such, this version is no longer the Accepted Manuscript, but it is not yet the definitive Version of Record; we are providing this early version to give early visibility of the article. Please note that Elsevier's sharing policy for the Published Journal Article applies to this version, see: https://www.elsevier.com/about/policies-and-standards/sharing#4-published-journal-article. Please also note that, during the production process, errors may be discovered which could affect the content, and all legal disclaimers that apply to the journal pertain.

© 2025 Published by Elsevier B.V.



Fabrication of MIP-201 Membrane with Excellent Stability for High-

Efficiency Uranium Separation from Seawater

Yue Zhang a, Jiaxin Liu b, Shishi Du c, Tingting Wang a, Meixi Yan a, Sixing Chen a,

Sujing Wang ^d, Xin Zheng ^c, Jing Ma ^{b,*}, Shin-ichiro Noro ^{c,*}, Yi Liu ^{a,e,*}

^a State Key Laboratory of Fine Chemicals, Frontiers Science Center for Smart Materials, School of

Chemical Engineering, Dalian University of Technology, Dalian 116024, China

^b China Nuclear Power Engineering Company Limited, Beijing 100840, China

^c Faculty of Environmental Earth Science, Hokkaido University, Sapporo 060-0810, Japan

d Hefei National Research Center for Physical Sciences at the Microscale, Suzhou Institute for Advanced

Research, Laboratory of Spin Magnetic Resonance, University of Science and Technology of China,

Hefei 230026, China

e Dalian Key Laboratory of Membrane Materials and Membrane Processes, Dalian University of

Technology, Dalian 116024, China

* Corresponding author:

E-mail: diligenliu@dlut.edu.cn (Yi Liu);

E-mail: noro@ees.hokudai.ac.jp (Shin-ichiro Noro);

E-mail: majing@cnpe.cc (Jing Ma).

Abstract

Uranium separation from seawater represents a promising approach for overcoming

uranium resource shortage. In this study, we fabricated an MIP-201 membrane with

exceptional long-term stability in uranium-containing environments for high-efficiency

uranium separation from seawater. Benefiting from 10.5 Å-sized pores, the UO₂²⁺

rejection rate reached 98.5%, which was significantly higher than smaller-sized metal

ions (e.g. 2-7% for K⁺, Na⁺, Ca²⁺ and Mg²⁺); moreover, our membrane exhibited ideal

Fe³⁺/UO₂²⁺ selectivity of 57.2, which represented the highest value in comparison with

the literature. Of particular note, owing to intrinsic framework robustness, our membrane maintained a steady UO_2^{2+} ion rejection rate of ~98% upon immersion in UO_2^{2+} -containing aqueous solution for over 30 days and ~97% in seawater for over 21 days, showing great potential in practical uranium separation from seawater.

Keywords: Metal-organic framework; Membrane; MIP-201; Nanofiltration; Uranium extraction



1. Introduction

With increasing concerns on global warming, nuclear power has been considered as a sustainable and clean source of energy instead of fossil fuels [1, 2]. However, limited amount of land-based uranium resources is incapable of meeting the growing demand of nuclear industry. Fortunately, uranium resource reserved in oceans is ~1,000 times more than in land-based ores [3, 4], potentially addressing the issue of uranium scarcity. Nonetheless, the complex composition of seawater poses a grand challenge for highefficiency uranium purification [5-8]. On the one hand, a large number of interfering metal ions co-exist in seawater, such as Fe³⁺, Ca²⁺, Mg²⁺, K⁺ and Na⁺, rendering highefficiency separation of UO₂²⁺ ions very challenging; on the other hand, the salinity of

seawater (3.2-4.0 wt.%) is $\sim 10^6$ times higher than UO₂²⁺ ions [9-11], significantly hindering high-efficiency enrichment of trace amount of uranium (~ 3.3 mg/t) from seawater [12, 13].

Diverse protocols, including adsorption [7, 14-17], photocatalysis [18-25], ion exchange [26-28], solvent extraction [29-31], and electrochemical precipitation [32-34], have been employed for uranium separation from seawater [35, 36]. Among them, membrane separation has received increasing attention due to easy operation, environmental friendliness, high efficiency, and low energy requirement [37-39]. Aiming to achieve high-efficiency uranium separation from seawater, however, accurate discrimination of UO₂²⁺ ions from co-existing interfering ions is indispensable. Fortunately, the kinetic diameter of hydrated UO₂²⁺ ions is 11.6 Å, which is much larger than other co-existing hydrated metal ions with kinetic diameters commonly falling below 9.1 Å [40-42]. Therefore, it is necessary to pursue molecular sieves with pore size of 9.1-11.6 Å.

Metal-organic framework (MOF), which is composed of regularly arranged organic ligands and metal ions/metal-oxo clusters [43-47], has been deemed as ideal candidate for precise molecular sieving because of its tuneable pore size, rich functional groups and high surface areas [37, 48-51]. Because of the higher Zr-O bonding energy (776 kJ·mol⁻¹) and coordination number (6-connected), Zr-MOF materials (e.g., UiO-66, MIP-200 and MIP-201) are anticipated to exhibit superior water and chemical stability, facilitating long-term operation under seawater environments [52, 53]. Among them, UiO-66 exhibits a pore size of ~6.0 Å [54], which is smaller than the hydrated ionic

diameters of major metal ions (e.g., K⁺, Na⁺, Ca²⁺, Mg²⁺) in seawater, while MIP-200 possesses a larger pore size of ~13 Å, which exceeds the hydrated ionic diameter of UO₂²⁺ ions, making them impossible to achieve accurate uranium separation from seawater[55, 56]. In contrast, MIP-201, consisting of Zr₆-oxo cluster secondary building units (SBUs) and tetra-carboxylate linkers (5,5'-methylenediisophthalic acid, H₄mdip), possesses an accessible pore size of 10.5 Å (Fig. S1a-d and S2b) which just falls between hydrated kinetic diameters of UO₂²⁺ ions and other co-existing metal ions in natural seawater, making it a promising membrane candidate for high-efficiency uranium separation from seawater.

In this study, we pioneered epitaxial growth of MIP-201 membrane on tubular porous α -Al₂O₃ substrate (illustrated in Fig. 1). First, MIP-201 seeds were synthesized by using ZrCl₄ as metal source. Second, MIP-201 seeds were deposited on porous α -Al₂O₃ tube at room temperature. Third, epitaxial growth was conducted to seal the open space in the seed layer. Benefiting from the 10.5 Å-sized pores, our membrane exhibited UO₂²⁺ ion rejection rate of 98.5%; in contrast, rejection rates of mono- and di-valent metal ions were below 7%. Of particular note, ideal selectivity of the Fe³⁺/UO₂²⁺ ion pair reached 57.2, which represented the highest value reported in the literature (Table S1). Long-term operation stability test indicated that our membrane could maintain uranium rejection rate of ~98% in aqueous solution for over 30 days and ~97% in seawater for over 21 days, showing great potential in practical uranium separation from seawater. Furthermore, our MIP-201 membrane still maintained the UO₂²⁺ ion rejection rate of

~97% under high HNO₃ concentration conditions, demonstrating excellent and stable separation performance.

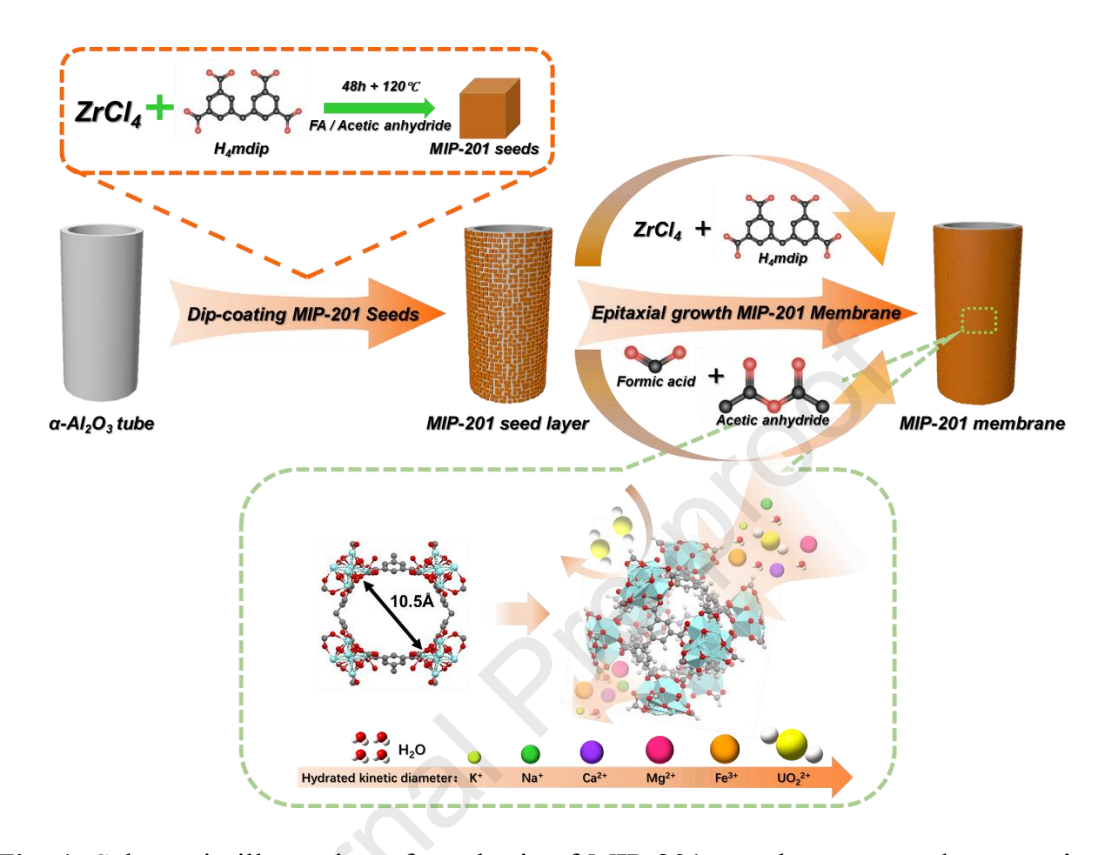


Fig. 1. Schematic illustration of synthesis of MIP-201 membrane towards separation uranium from nature seawater.

2. Methods

2.1 Preparation of MIP-201 seeds

5,5'-Methylenediisophthalic acid (H₄mdip, 125 mg, 0.36 mmol, Shanghai Tensus Bio-tech Co. Ltd.) was added into a binary solvent comprising acetic anhydride (3.75 mL) and formic acid (FA, 2.5 mL), followed by sonication at 5 °C for 10 min. Subsequently, ZrCl₄ (203 mg, 0.87 mmol) was added dropwise to the above solution. After sonication for 10 min at 5 °C, the above solution was transferred to a 30 mL Teflon-lined autoclave and solvothermally treated at 120 °C under static conditions for

48 h. Finally, MIP-201 seeds were washed with ethanol and dried at 60 °C overnight.

2.2 Preparation of MIP-201 seed layer

Dip-coating was employed to deposit MIP-201 seeds. MIP-201 seed suspension (6 mg/mL) was prepared by adding 180 mg of MIP-201 seeds in 30 mL methanol (MeOH), followed by addition of 30 μ L of 10 mM polyvinylpyrrolidone (PVP) solution (N,N-dimethylformamide (DMF) solvent) in the suspension. Subsequently, porous α -Al₂O₃ tube was immersed in above MIP-201 seed-containing suspension for 20 s and slowly lifted out. The above process was repeated twice. Finally, as-prepared MIP-201 seed layer was dried at 60 °C overnight.

2.3 Preparation of MIP-201 membrane

100 mg H₄mdip was added into binary solvent comprising 10 mL Formic acid and 15 mL Acetic anhydride, followed by sonication for 10 min at 5 °C. Subsequently, 203 mg of ZrCl₄ was added into above suspension. The suspension was poured into a 60 mL Teflon-lined autoclave where the MIP-201 seed layer was vertically placed. In the next step, Teflon-lined autoclave was treated at 120 °C under static conditions for 48 h. Finally, the MIP-201 membrane was washed with de-ionized water to remove residual formic acid and acetic anhydride in the membrane.

3. Result and discussion

3.1 Preparation of MIP-201 seeds

The first step referred to the preparation of MIP-201 seeds, which could be obtained through mixing ligand (H₄mdip), metal source (ZrCl₄), and modulator (formic acid and

acetic anhydride), followed by solvothermal growth. Nonetheless, undesired MIP-200 impure phase, featuring 3D Kagometype framework with 13Å-sized separated hexagonal pores and 6.8 Å-sized triangular channels pores along the c-axis, may be simultaneously generated [55, 56]. Fortunately, our results revealed that MIP-200 nucleation could be effectively suppressed through precisely controlling the concentration of acetic anhydride and FA in the precursor solution. To be specific, increasing the concentration of acetic anhydride and FA favored the formation of MIP-200 phase and vice versa (Fig. S3a-f). Owing to higher concentration of deprotonating reagents, the concentration of intermediates will be lower through coordinative interaction between Zr (IV) cations and monocarboxylic acid modulators, resulting in effective suppression of MIP-201 nucleation and growth, and therefore, formation of MIP-200 impure phase [57-60]. Under optimized reaction conditions, cubic-shaped pure-phase MIP-201 crystals with size distribution in the range of 0.7 and 1.1 µm could be obtained (Fig. 2a-b and S4-5). N₂ adsorption/desorption isotherms indicated that their micropore volume and BET surface areas reached 0.30 cm³·g⁻¹ and 575 m²·g⁻¹ (Fig. S2a), which was consistent with reported literature [61]. Based on the BET results, the pore size of obtained MIP-201 reached 10.5 Å (Fig. S2a), which was coincident with the simulation results (Fig. S2b).

Considering high salinity, complex composition, and varying temperature of seawater, framework robustness of MIP-201 seeds was further evaluated through immersion them in aqueous solution with varying pH values (1~4 and 10) and temperatures. As show in Fig. S6, surface morphology of MIP-201 crystals did not

change under above harsh conditions. XRD patterns and FT-IR spectra further demonstrated that not only their framework structure remained intact but also functional groups were unchanged (Fig. S7 and S8). In addition, TGA data indicated that there was no significant weight loss up to 400 °C, which proved that MIP-201 seeds had excellent thermal stability (Fig. S9). Exceptional chemical and thermal stability of MIP-201 crystals made it ideal membrane candidate to survive in harsh operation conditions of uranium separation from seawater.

3.2 Preparation of MIP-201 seeds layer and membrane.

Subsequently, we attempted to deposit MIP-201 seeds on porous α -Al₂O₃ tube through dip-coating. Our results indicated that the addition of PVP in precursor solution represented the key factor to maintain uniformity of MIP-201 seed layer, owing to weakened interactions among MIP-201 seeds and enhanced dispersion in suspension [62, 63]. As shown in Fig. S10, MIP-201 seeds could be uniformly deposited on the substrate upon keeping seed concentration in the range of 4 ~ 8 mg/mL; while further increasing seed concentration led to their severe aggregation on the substrate surface. SEM images and XRD pattern revealed that the MIP-201 seed layer prepared was 3.8 μ m-thick with no preferred orientation under optimized deposition conditions (Fig. 2c-d and 3).

Finally, epitaxial growth was employed to close the open space in seed layers. Experimental data showed that the concentration H4mdip ligands exerted significant influence on membrane continuity. For instance, maintaining H4mdip concentration of

4 mg/mL resulted in the growth of well-intergrown MIP-201 membrane with a thickness of 4.9 μm (Fig. 2e and 2f), while XRD pattern showed that as-prepared membrane belonged to pure MIP-201 phase (Fig. 3). Further increasing the concentration of H4mdip to 5 mg/mL led to simultaneous generation of MIP-200 impure crystallites in the membrane (Fig. S11 and S12a); in contrast, reducing the H4mdip concentration to 3 mg/mL resulted in the formation of substantial grain boundary defects in the membrane, owing to insufficient nutrient supply during epitaxial growth (Fig. S12a-c). As shown in Fig. S12d-f, the surface of as-prepared membrane is hydrophilic, facilitating enhanced water permeance. It should be noted that even after immersion in aqueous solutions with varying pH values for 24 h (1~4 and 10), room-temperature water for 720 h, and boiling water for 24 h (Fig. S13), diffraction peaks derived from MIP-201 membranes remained prominent, implying that undesired lattice distortion or degradation did not occur [64, 65], which was advantageous for long-term operation of membranes under harsh environments.

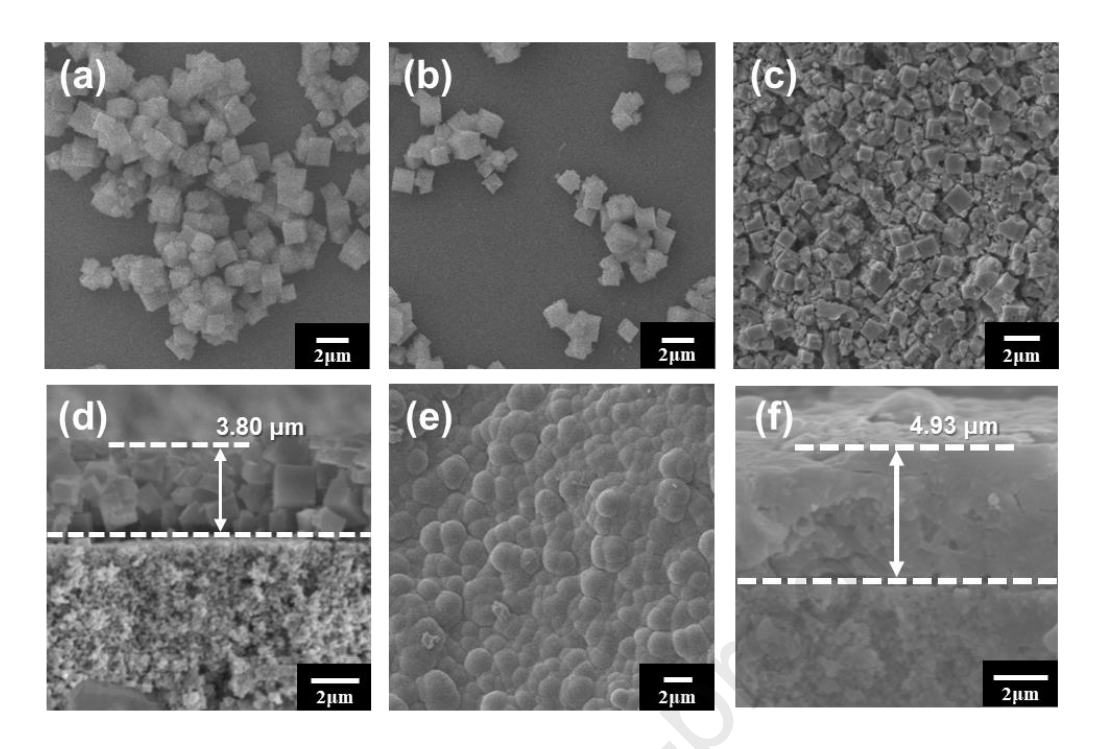


Fig. 2. SEM images of (a,b) MIP-201 seeds, (c,d) MIP-201 seed layer, and (e,f) MIP-201 membrane.

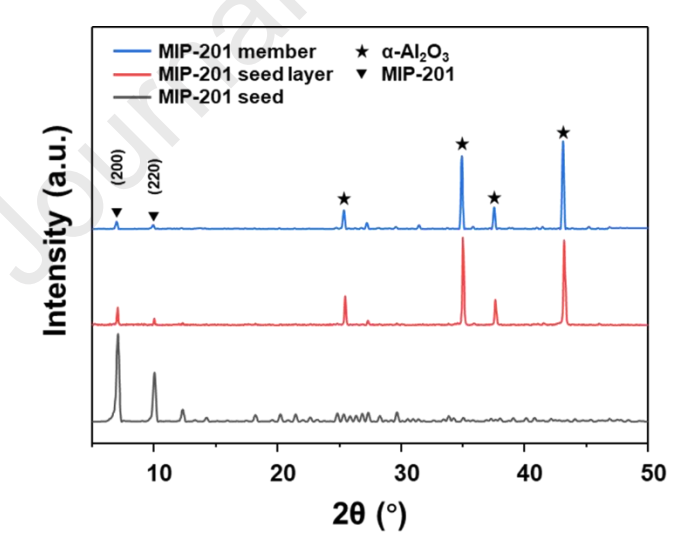


Fig. 3. XRD patterns of MIP-201 seeds, MIP-201 seed layer, and MIP-201 membrane, respectively.

3.3 Ion rejection tests of MIP-201 membrane.

Prior to the ion rejection test, the permeation behavior of DI water through MIP-201 membrane was studied. Owing to a pore size of 10.5 Å, its water permeance reached 7.1 L·m⁻²·h⁻¹·bar⁻¹, which was higher than most water-stable MOF membranes [66]. Hydrated kinetic diameters of metal ions were found to follow the order: K^+ (6.6 Å) < $Na^{+}(7.2 \text{ Å}) < Ca^{2+}(8.2 \text{ Å}) < Mg^{2+}(8.6 \text{ Å}) < Fe^{3+}(9.1 \text{ Å}) < UO_2^{2+}(11.6 \text{ Å}) [40-42, 54, 1]$ 67]. Since the pore size of MIP-201 just fell between hydrated diameters of UO₂²⁺ ions and other metal ions, accurate screening of UO22+ ions from seawater was anticipated to be achieved (Fig. 4). As shown in Fig. 5a, the rejection rate of UO22+ ions of our membrane reached 98.5%, which was much higher those of K⁺ (2.4 %), Na⁺ (2.9 %), Ca^{2+} (5.5 %), Mg^{2+} (7.0 %) and Fe^{3+} ions (28.0 %), implying that size-based exclusion represented the dominant mechanism for hydrated metal ion rejection; correspondingly, ideal selectivity of K^+/UO_2^{2+} , Na^+/UO_2^{2+} , Ca^{2+}/UO_2^{2+} , Mg^{2+}/UO_2^{2+} and Fe^{3+}/UO_2^{2+} ion pairs reached 77.6, 77.3, 75.9, 75.3 and 57.2, respectively (Fig. 5b), demonstrating that our membrane enabled effective separation of UO22+ ions from other co-existing metal ions. Of particular note, our membrane exhibited higher Fe³⁺/UO₂²⁺ selectivity in comparison with previous literatures (Fig. S14 and Table S1), which could be attributed to its appropriate pore size; simultaneously, water permeances were found to be negatively correlated with hydrated kinetic diameters of metal ions as follows: K⁺ (6.98 $L \cdot m^{-2} \cdot h^{-1} \cdot bar^{-1}$ > Na^{+} (6.42 $L \cdot m^{-2} \cdot h^{-1} \cdot bar^{-1}$) > Ca^{2+} (6.28 $L \cdot m^{-2} \cdot h^{-1} \cdot bar^{-1}$) > Mg^{2+} (6.25 $L \cdot m^{-2} \cdot h^{-1} \cdot bar^{-1}$ > UO_2^{2+} (6.15 $L \cdot m^{-2} \cdot h^{-1} \cdot bar^{-1}$) > Fe^{3+} (5.94 $L \cdot m^{-2} \cdot h^{-1} \cdot bar^{-1}$) (Fig. 5a).

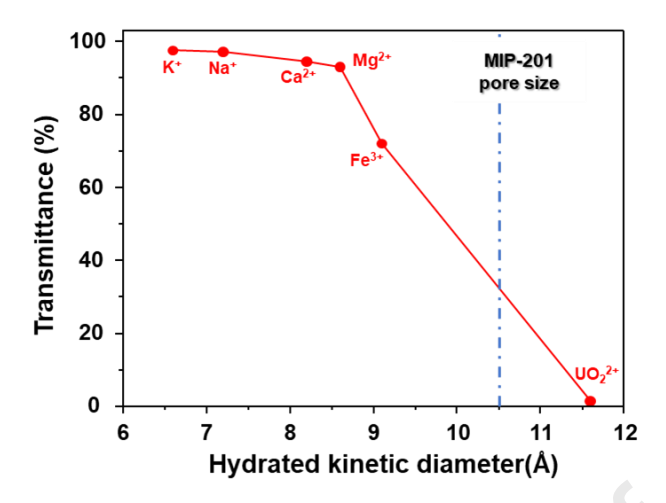


Fig. 4. Metal ion transmittance rate of MIP-201 membrane as a function of hydrated kinetic diameters of various metal ions.

We further evaluated the performance of binary metal ion rejection of the membrane. As shown in Fig. 5c, compared with single metal ions, there was considerable increase of rejection rates of hydrated metal ions under the conditions of the coexistence of interfering metal ions (e.g., K*: 18.5%; Na*: 20.7%; Ca²+: 21.0%; Mg²+: 23.1%; Fe³+: 51.8%). This may be due to strong coupling effects (e.g., coulombic electrostatic potential and hard-core interaction) between them and their competitive diffusion in nanochannels, leading to higher free energy barriers for ion permeation (Fig. S15 and Table S2) [68, 69]. To be specific, the selectivity of K*/UO2²+, Na*/UO2²+, Ca²+/UO2²+, Mg²+/UO2²+ and Fe³+/UO2²+ ion pairs reached 58.82, 44.78, 37.08, 32.18 and 29.05, respectively (Fig. 5d) with water permeance remaining largely unchanged (6.34, 6.33, 6.20, 5.97 and 5.25 L·m²-h¹-l·bar-¹) (Fig. 5e). In comparison with previous literature (Fig. 5f), our membrane displayed efficient UO2²+, n = 1, 2, 3) with negligible decay

in water permeance, which was advantageous for maintaining superior performance in harsh environments like seawater (Table S3 and S4).

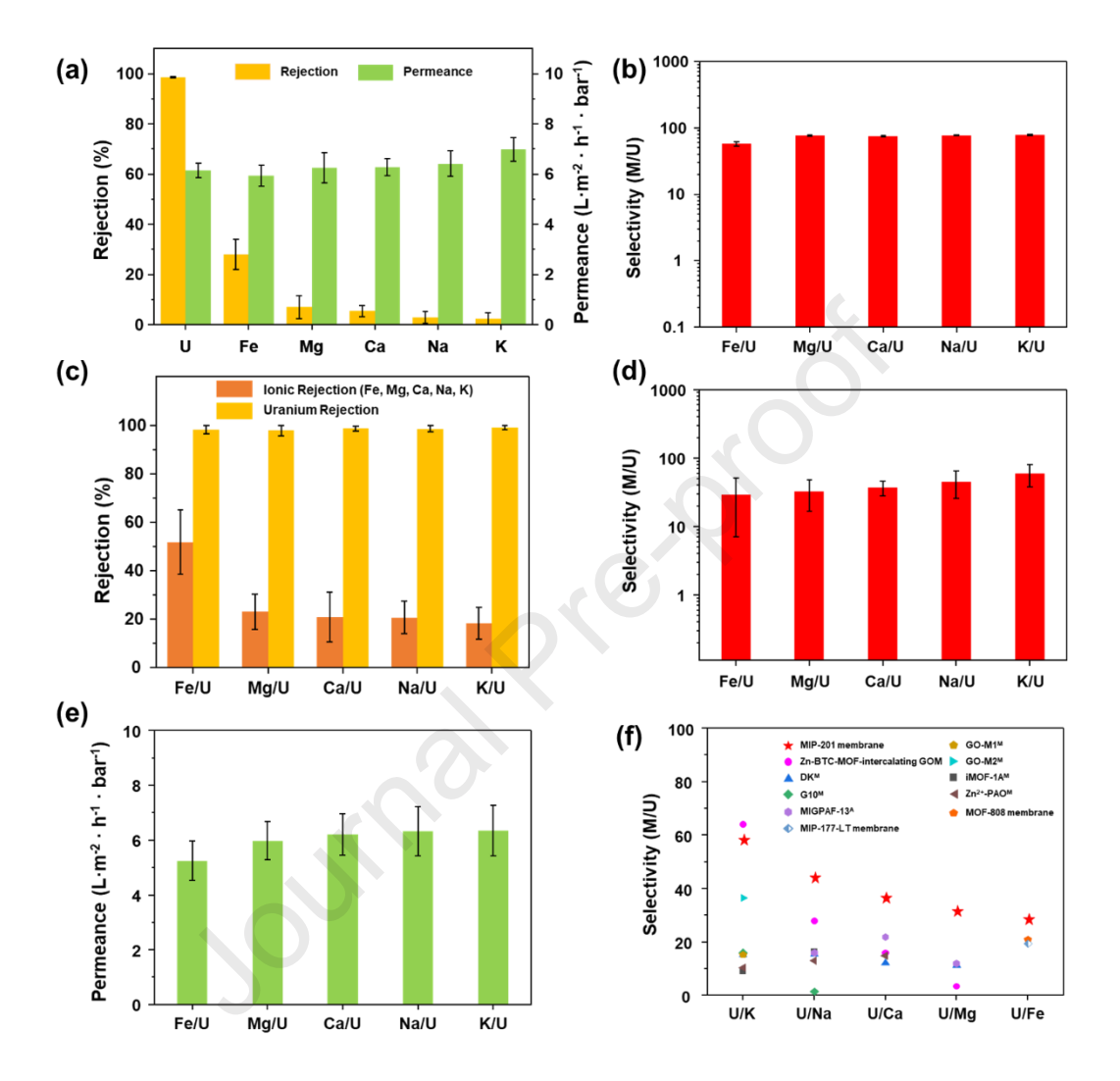


Fig. 5. (a) Single metal ion rejection capacity of MIP-201 membrane. (b) Ideal SF of Mⁿ⁺ (n=1, 2, 3)/UO₂²⁺ ion pairs of MIP-201 membrane. (c) Ion rejection rate, (d) water permeance, and (e) Mⁿ⁺ (n=1, 2, 3)/UO₂²⁺ SF of MIP-201 membrane in the presence of interfering metal ions. (f) Comparison of Mⁿ⁺ (n=1, 2, 3)/ UO₂²⁺ SF of MIP-201 membrane with those reported in literatures (Table S3 and S4).

Aiming at practical applications, we further investigated uranium rejection capacity

of MIP-201 membrane with seawater at the feed side. Prior to metal ion rejection test, the stability of our MIP-201 membrane in natural seawater was evaluated. As shown in Fig. S16, surface morphology of MIP-201 membrane did not change after immersion in natural seawater over 10 days; simultaneously, XRD patterns demonstrated that its framework structure remained intact, confirming its excellent stability in natural seawater. According to the literature, uranium in seawater primarily existed in form of UO2²⁺ ions [70, 71]. The contents of major metal ions collected from the seawater were as follow (Fig. 6a): Na⁺ (~9336 ppm) > Mg²⁺ (~873 ppm) > K⁺ (~357 ppm) ~ Ca²⁺ $(\sim 357 \text{ ppm}) > \text{Fe}^{3+} (\sim 0.0041 \text{ ppm}) > \text{UO}_2^{2+} (\sim 0.003 \text{ ppm}) [40]. \text{ Metal ion rejection test}$ results indicated that the rejection rate of UO22+ ions reached 98.0%, which remained comparable with that of single UO22+ ions; simultaneously, rejection rates of other coexisting metal ions only slightly increased (e.g., K⁺: 20.3%; Na⁺: 20.4%; Ca²⁺: 21.0%; Mg²⁺: 23.2%; Fe³⁺: 53.7%) (Fig. 6b). As a result, our membrane still exhibited decent selectivity towards $K^{+/}UO_2^{2+}$ (34.51), $Na^{+/}UO_2^{2+}$ (32.99), $Ca^{2+/}UO_2^{2+}$ (31.88), $Mg^{2+}/UO_{2^{2+}}$ (31.40) and $Fe^{3+}/UO_{2^{2+}}$ (18.35) ion pairs (Fig. 6c), demonstrating that high salinity environment did not compromise the separation performance of MIP-201 membrane. In addition, considering the possible impact of vanadium anions (hydrated kinetic diameter ~ 0.9 nm [48, 72-75]) on uranium separation from seawater, vanadium rejection test was conducted. As shown in Fig. S17, a VO₃-/UO₂²⁺ separation factor (SF_{V/U}) of 13.32 was achieved under natural seawater conditions, indicating that the presence of vanadium anions did not pose significant interference to high-efficiency uranium extraction from seawater. It should be noted that in spite of the presence of

organisms such as algae in seawater, water permeance of MIP-201 membrane still reached 4.78 L·m⁻²·h⁻¹·bar⁻¹ (Fig. 6d), showing great potential in high-efficiency separation uranium from nature seawater.

Natural seawater also contains abundant anions (e.g., Cl-). Therefore, we further investigated the uranium separation performance in the presence of anions. Due to its smaller hydrated dynamic diameter (6.6 Å) compared with the pore size of MIP-201 (10.5 Å) [40-42], our membrane exhibited a low Cl⁻ anions rejection rate of only 2.44% (Fig. S18a). Subsequently, the uranium rejection test was conducted with the coexistence of Cl⁻ anions. As shown in Fig. S18c, its UO₂²⁺ ion rejection rate remained essentially identical with single UO₂²⁺ ion solution, demonstrating that anions in seawater had negligible impact on the uranium separation performance of MIP-201 membrane. It should be noted that since the hydrated kinetic diameters of Cl⁻ anions and K⁺ ions are identical, the rejection rate and separation factor (SF) are also essentially the same, which is in good agreement with the proposed size-sieving mechanism (Fig. S18b and S18c). We further investigated the effect of the presence of larger anions (e.g., SO₄²- with hydrated dynamic diameter of 7.6 Å [41, 42]) on uranium separation performance. The membrane exhibited a low SO₄²- rejection rate of 4.03% in the absence of SO_4^{2-} anions. As shown in Fig. S19, the UO_2^{2+} ion rejection rate remained largely unchanged (98.95%) in the presence of 8.03 mM UO22+ ions, indicating that the presence of larger-sized SO₄²⁻ anions had negligible influence on the uranium separation performance of obtained MIP-201 membrane".

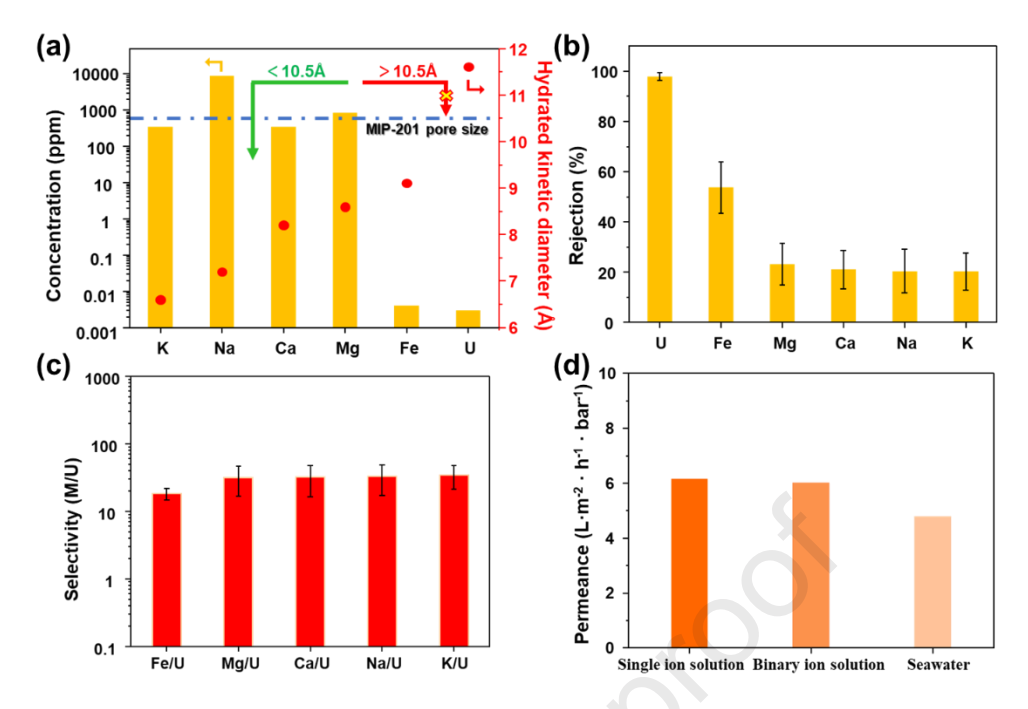


Fig. 6. (a) Concentration of major metal ions present in Yellow Sea. (b) Ion rejection rate and (c) M^{n+} (n=1, 2, 3)/ UO_2^{2+} selectivity of MIP-201 membrane with seawater at the feed side. (d) Water permeance of MIP-201 membrane with different solutions at the feed side.

3.4 Operation Stability of MIP-201 Membrane.

Finally, we evaluated cycling and long-term operation stability of MIP-201 membrane. As shown in Fig. 7a, in terms of single uranium aqueous solution, the UO2²⁺rejection rate could be maintained at ~97% with water permeance of ~6 L·m⁻²·h⁻¹·bar⁻¹ even after 10 test cycles; simultaneously, the rejection rate of UO2²⁺ ions was ~98% with no noticeable decline during continuous operation for over 30 days (Fig. 7b), revealing excellent long-term operational stability. Moreover, relevant stability test was conducted by using aqueous HNO3 solution containing uranium at the feed side. As shown in Fig. S20a, the MIP-201 membrane maintained UO2²⁺ ion rejection rate

~97% for 12 days even on the co-existence of 50 mM HNO₃. Furthermore, the UO₂²⁺ ion rejection rate of MIP-201 membrane was not significantly affected after 24 hours of immersion in water at 40 °C (Fig. S20b). The above results convincingly demonstrated superior pH and temperature stability of our membrane. Adaptability of MIP-201 membrane to non-treated seawater was verified further [76, 77]. As shown in Fig. 7c, during continuous operation for 7 days, our membrane maintained steady rejection rate of ~97% for UO₂²⁺ ions with rejection rates for mono- and di-valent metal ions falling below 35%; in contrast, its water permeance gradually declined over time, reaching a steady value of ~1.8 L·m⁻²·h⁻¹·bar⁻¹ after two days (Fig. S21). This could be reasonably interpreted by concentration polarization and membrane fouling [78-81].

Fortunately, water permeance could be recovered to 86% of the initial value after the first washing and 83% of the initial value after the second washing (Fig. S22a); simultaneously, our membrane maintained a rejection rate of ~97% for UO₂²⁺ ions with rejection rates of mono- and di-valent metal ions falling below 40%, which was almost identical with that of freshly prepared membrane (Fig. S22b). Excellent and stable performance of MIP-201 membrane made it advantageous for practical applications in uranium separation from seawater (Fig. 7d).

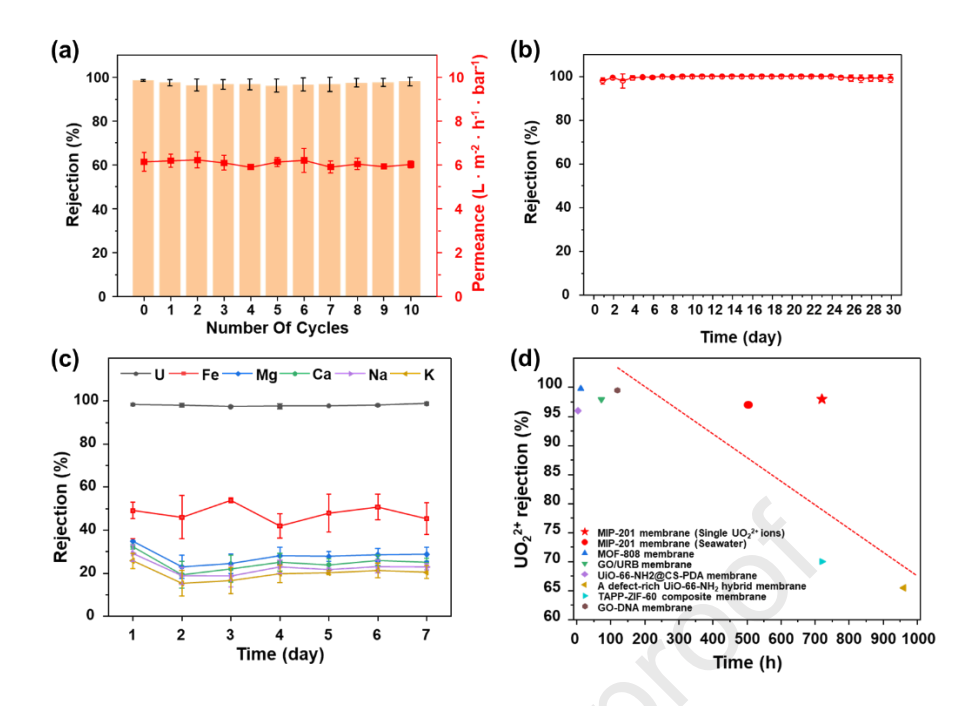


Fig. 7. (a) Dependence of UO₂²⁺ rejection rate and water permeance of MIP-201 membrane on cycle number in terms of single uranium aqueous solution. Operation stability of MIP-201 membrane in (b) single uranium aqueous solution and (c) seawater. (d) Operation stability of MIP-201 membrane in comparison with the previous literature (Table S5).

4. Conclusion

In this study, MIP-201 tubular membrane with excellent water and chemical stability was first prepared. Relying on 10.5 Å-sized nano-channels, our membrane exhibited 98.5% rejection rate for UO₂²⁺ ions while keeping rejection rates for smaller-sized metal ions in the range of 2-7%. Of particular note, its ideal Fe³⁺/UO₂²⁺ selectivity reached 57.2, representing the highest value reported in the literature. Even under harsh seawater conditions, the rejection rate of UO₂²⁺ ions remained over 98% with water permeance largely unchanged. Furthermore, our membrane showed excellent cycling

stability and long-term operation stability in uranium-containing aqueous solution, showing great promise for practical uranium separation from seawater.

CRediT authorship contribution statement

Yue Zhang: Writing — original draft & review, Methodology, Investigation, Formal analysis, Conceptualization. Jiaxin Liu: Writing — review, Investigation. Shishi Du: Formal analysis. Tingting Wang: Investigation. Meixi Yan: Investigation. Sixing Chen: Writing — review. Sujing Wang: Supervision. Xin Zheng: Writing — review. Jing Ma: Writing — review & editing, Supervision. Shin-ichiro Noro: Writing — review, Supervision. Yi Liu: Writing — review & editing, Supervision, Resources, Funding acquisition, Conceptualization.

Declaration of competing interest

The authors declare that they have no known competing financial interests or personal relationships that could have appeared to influence the work reported in this paper.

Acknowledgments

The authors are grateful to National Natural Science Foundation of China (22478056), JSPS KAKENHI (JP12345678), Xing Yuan program of China National Nuclear Corporation (8208 of CNPE), Liaoning Province Funds for Distinguished Young Scholars (2024JH3/50100002), Science Fund for Creative Research Groups of the National Natural Science Foundation of China (22021005), Liaoning Binhai Laboratory (LBLG-2024-07), State Key Laboratory of Catalysis (2024SKL-A-003),

National Key Research and Development Program of China (2023YFB3810700), and Science and Technology Innovation Fund of Dalian (2024JJ12GX027) for the financial support.

Appendix A. Supplementary data

Supplementary data to this article can be found online.

References

- [1] L. Zeyu, X. Yi, W. Yifan, H.U. Tongyang, Y.E. Gang, C. Jing. Recent advances in sorbent materials for uranium extraction from seawater. J Tsinghua Univ(Sci Technol). 61 (2021) 279-301.
- [2] W. Dan. Interpretation of the 13th Five-Year Development Plan in Support of Nuclear Power Development. Chinese Nuclear Power. 10 (2017) 157-160.
- [3] C.W. Abney, R.T. Mayes, T. Saito, S. Dai, O.R.T.U. Oak Ridge National Laboratory ORNL. Materials for the Recovery of Uranium from Seawater. Chem. Rev. 117 (2017) 13935-14013.
- [4] C.X. Zhao, J.N. Liu, B.Q. Li, D. Ren, X. Chen, J. Yu, Q. Zhang. Multiscale Construction of Bifunctional Electrocatalysts for Long-Lifespan Rechargeable Zinc-Air Batteries. Adv. Funct. Mater. 30 (2020) 2003619.
- [5] Y. Wu, Y. Xie, X. Liu, Y. Li, J. Wang, Z. Chen, H. Yang, B. Hu, C. Shen, Z. Tang, Q. Huang, X. Wang. Functional nanomaterials for selective uranium recovery from seawater: Material design, extraction properties and mechanisms. Coord. Chem. Rev. 483 (2023) 215097.
- [6] B.K. Singh, M. Asim, Z. Salkenova, D. Pak, W. Um. Engineered Sorbents for Selective Uranium Sequestration from Seawater. ACS ES&T Water. 4 (2024) 325-345.
- [7] Y. Song, B. Deng, K. Wang, Y. Zhang, J. Gao, X. Cheng. Highly-efficient adsorbent materials for uranium extraction from seawater. J. Environ. Chem. Eng. 12 (2024) 113967.
- [8] A. Krestou, D. Panias. Uranium (VI) speciation diagrams in the UO₂²⁺/CO₃²⁻/H₂O system at 25°C. Eur. J. Miner. Process. Environ. 4 (2004) 113-129.
- [9] D. Zhang, L. Fang, L. Liu, B. Zhao, B. Hu, S. Yu, X. Wang. Uranium extraction from seawater by novel materials: A review. Sep. Purif. Technol. 320 (2023) 124204.

- [10] C. Xing, B. Bernicot, G. Arrachart, S. Pellet-Rostaing. Application of ultra/nano filtration membrane in uranium rejection from fresh and salt waters. Sep. Purif. Technol. 314 (2023) 123543.
- [11] F. Endrizzi, C.J. Leggett, L. Rao. Scientific Basis for Efficient Extraction of Uranium from Seawater. I: Understanding the Chemical Speciation of Uranium under Seawater Conditions. Ind. Eng. Chem. Res. 55 (2016) 4249-4256.
- [12] A.P. Ladshaw, S. Das, W.P. Liao, S. Yiacoumi, C.J. Janke, R.T. Mayes, S. Dai, C. Tsouris. Experiments and Modeling of Uranium Uptake by Amidoxime-Based Adsorbent in the Presence of Other Ions in Simulated Seawater. Ind. Eng. Chem. Res. 55 (2016) 4241-4248.
- [13] N. He, H. Li, L. Li, C. Cheng, X. Lu, J. Wen, X. Wang. Polyguanidine-modified adsorbent to enhance marine applicability for uranium recovery from seawater. J. Hazard. Mater. 416 (2021) 126192.
- [14] X. Ye, R. Chi, Z. Wu, J. Chen, Y. Lv, C. Lin, Y. Liu, W. Luo. A biomass fiber adsorbent grafted with phosphate/amidoxime for efficient extraction of uranium from seawater by synergistic effect. J. Environ. Manage. 337 (2023) 117658.
- [15] L. Kuo, H. Pan, C.M. Wai, M.F. Byers, E. Schneider, J.E. Strivens, C.J. Janke, S. Das, R.T. Mayes, J.R. Wood, N. Schlafer, G.A. Gill. Investigations into the Reusability of Amidoxime-Based Polymeric Adsorbents for Seawater Uranium Extraction. Ind. Eng. Chem. Res. 56 (2017) 11603-11611.
- [16] Y. Li, Y. Zheng, Z. Ahamd, L. Zhu, J. Yang, J. Chen, Z. Zhang. Strategies for designing highly efficient adsorbents to capture uranium from seawater. Coord. Chem. Rev. 491 (2023) 215234.
- [17] X. Chang, P. Hu, H. Liu, Z. Lv, J. Yang, J. Wang, Z. Li, L. Qian, W. Wu. ZIF-8 modified graphene oxide/sodium alginate 3D elastic spheres for uranium trapping in seawater. Desalination. 549 (2023) 116371.
- [18] F. Yu, C. Li, W. Li, Z. Yu, Z. Xu, Y. Liu, B. Wang, B. Na, J. Qiu. Π-Skeleton Tailoring of Olefin-Linked Covalent Organic Frameworks Achieving Low Exciton Binding Energy for Photo-Enhanced Uranium Extraction from Seawater. Adv. Funct. Mater. 34 (2024) 2307230.
- [19] S. Zhao, T. Feng, M. Cao, T. Liu, Y. Yuan, N. Wang. Ferrocene-based 2D metal-organic framework nanosheet for highly efficient photocatalytic seawater uranium recovery. Chem. Eng.

- J. 498 (2024) 155228.
- [20] T. Liu, A. Gu, T. Wei, M. Chen, X. Guo, S. Tang, Y. Yuan, N. Wang. Ligand-Assistant Iced Photocatalytic Reduction to Synthesize Atomically Dispersed Cu Implanted Metal-Organic Frameworks for Photo-Enhanced Uranium Extraction from Seawater. Small. 19 (2023) e2208002.
- [21] C. Chen, L. Fei, B. Wang, J. Xu, B. Li, L. Shen, H. Lin. MOF-Based Photocatalytic Membrane for Water Purification: A Review. Small. 20 (2024) 2305066.
- [22] X. Ma, K.R. Meihaus, Y. Yang, Y. Zheng, F. Cui, J. Li, Y. Zhao, B. Jiang, Y. Yuan, J.R. Long, G. Zhu. Photocatalytic Extraction of Uranium from Seawater Using Covalent Organic Framework Nanowires. J. Am. Chem. Soc. 146 (2024) 23566-23573.
- [23] W. Wang, Q. Luo, J. Li, Y. Li, R. Wu, Y. Li, X. Huo, N. Wang. Single-atom tungsten engineering of MOFs with biomimetic antibiofilm activity toward robust uranium extraction from seawater. Chem. Eng. J. 431 (2022) 133483.
- [24] B. Zhang, X. Shan, J. Yu, H. Zhang, K. Tawfik Alali, Q. Liu, J. Zhu, J. Yu, J. Liu, R. Li, J. Wang. Facile synthesis of TiO2-PAN photocatalytic membrane with excellent photocatalytic performance for uranium extraction from seawater. Sep. Purif. Technol. 328 (2024) 125026.
- [25] F. Yu, Z. Zhu, S. Wang, Y. Peng, Z. Xu, Y. Tao, J. Xiong, Q. Fan, F. Luo. Tunable perylene-based donor-acceptor conjugated microporous polymer to significantly enhance photocatalytic uranium extraction from seawater. Chem. Eng. J. 412 (2021) 127558.
- [26] Y.S. Park, J. Lee, M.J. Jang, J. Yang, J. Jeong, J. Park, Y. Kim, M.H. Seo, Z. Chen, S.M. Choi. High-performance anion exchange membrane alkaline seawater electrolysis. J. Mater. Chem. A. 9 (2021) 9586-9592.
- [27] H. Li, S. Chen, Y. Song, H. Ding, Z. Li, H. Wu, F. Wang, H. Li, Z. Gao, H. Wang. Preparation of Antibioadhering Materials Containing Quaternary Phosphonium Salt for Uranium Extraction from Seawater. ACS Appl. Polym. Mater. 6 (2024) 3796-3804.
- [28] R.I. Foster, J.T.M. Amphlett, K. Kim, T. Kerry, K. Lee, C.A. Sharrad. SOHIO process legacy waste treatment: Uranium recovery using ion exchange. J. Ind. Eng. Chem. 81 (2020) 144-152.
- [29] G. Jegan, B. Sreenivasulu, A. Suresh, C.V.S. Brahmananda Rao, N. Sivaraman, G. Gopakumar. Experimental and theoretical studies on solvent extraction of uranium (VI) with

- hexapropyl and hexabutyl phosphoramide extractants. Solvent Extr. Ion Exch. 40 (2022) 312-332.
- [30] A. Abdeshahi, M.H. Sadeghi, D. Ghoddocy Nejad, M. Habibi Zare, M. Outokesh. Recovery of uranium from phosphate ore of Iran mine: Part II- solvent extraction of uranium from wet-process phosphoric acid. Nucl. Eng. Des. 421 (2024) 113093.
- [31] N. Tsutsui, Y. Ban, H. Sagawa, S. Ishii, T. Matsumura. Solvent Extraction of Uranium with N, N -Di(2-Ethylhexyl) Octanamide from Nitric Acid Medium. Solvent Extr. Ion Exch. 35 (2017) 439-449.
- [32] C. Liu, P. Hsu, J. Xie, J. Zhao, T. Wu, H. Wang, W. Liu, J. Zhang, S. Chu, Y. Cui. A half-wave rectified alternating current electrochemical method for uranium extraction from seawater. Nat. Energy. 2 (2017).
- [33] F. Chi, S. Zhang, J. Wen, J. Xiong, S. Hu. Highly Efficient Recovery of Uranium from Seawater Using an Electrochemical Approach. Ind. Eng. Chem. Res. 57 (2018) 8078-8084.
- [34] H. Feng, H. Dong, P. He, J. He, E. Hu, Z. Qian, J. Li, J. Li, W. Zhu, T. Chen. Nickel single atom mediated phosphate functionalization of moss derived biochar effectively enhances electrochemical uranium extraction from seawater. J. Mater. Chem. A. 12 (2024) 7795-7896.
- [35] L. Zhu, C. Zhang, F. Ma, C. Bi, R. Zhu, C. Wang, Y. Wang, L. Liu, H. Dong. Hierarchical Self-Assembled Polyimide Microspheres Functionalized with Amidoxime Groups for Uranium-Containing Wastewater Remediation. ACS Appl. Mater. Interfaces. 15 (2023) 5577-5589.
- [36] W. Cai, Y. Wang, L. Chen, Q. Luo, L. Xiong, Z. Zhang, L. Xu, X. Cao, Y. Liu. High-efficiency adsorptive removal of U(VI) on magnetic mesoporous carbon/Sr-doped hydroxyapatite composites. Colloid Surface A. 683 (2024) 132975.
- [37] B. MO, Y. ZHANG, G. LIU, G. LIU, W. JIN. Recent progress of metal-organic framework membranes for mono/divalent ions separation. CIESC Journal. 75 (2024) 1183-1197.
- [38] G. Zhao, Y. Zhang, Y. Li, G. Pan, Y. Liu. Positively charged nanofiltration membranes for efficient Mg²⁺/Li⁺ separation from high Mg²⁺/Li⁺ ratio brine. Adv. Membr. 3 (2023) 100065.
- [39] H.Y. Peng, S.K. Lau, W.F. Yong. Recent advances of thin film composite nanofiltration membranes for Mg²⁺/Li⁺ separation. Adv. Membr. 4 (2024) 100093.
- [40] M. Wu, J. Yan, T. Ji, K. Yu, Y. Sun, Y. Liu, X. Bai, Y. Liu, J. Liu, J. Ma, Y. Liu. Synthesis

- of (222)-oriented defect-rich MOF-808 membranes towards high-efficiency uranium rejection.

 J. Membr. Sci. 717 (2025) 123570.
- [41] B. Tansel. Significance of thermodynamic and physical characteristics on permeation of ions during membrane separation: Hydrated radius, hydration free energy and viscous effects. Sep. Purif. Technol. 86 (2012) 119-126.
- [42] B. Tansel, J. Sager, T. Rector, J. Garland, R.F. Strayer, L. Levine, M. Roberts, M. Hummerick, J. Bauer. Significance of hydrated radius and hydration shells on ionic permeability during nanofiltration in dead end and cross flow modes. Sep. Purif. Technol. 51 (2006) 40-47.
- [43] W.J. Koros, C. Zhang. Materials for next-generation molecularly selective synthetic membranes. Nat. Mater. 16 (2017) 289-297.
- [44] H.B. Park, J. Kamcev, L.M. Robeson, M. Elimelech, B.D. Freeman. Maximizing the right stuff: The trade-off between membrane permeability and selectivity. Science. 356 (2017).
- [45] D. Lee, S. Lee, I. Choi, M. Kim. Positional functionalizations of metal-organic frameworks through invasive ligand exchange and additory MOF-on-MOF strategies: A review. Smart Molecules. 2 (2024) e20240002.
- [46] L. Zhao, Y. Ren, X. Shi, H. Liu, Z. Yu, J. Gao, J. Zhao. Unveiling the unexpected sinking and embedding dynamics of surface supported Mo/S clusters on 2D MoS₂ with active machine learning. Smart Molecules. 3 (2025) e20240018.
- [47] Y. Wang, B. Yan, J. Liu, R. Wang, P. Rao, Y. Liu. Advances in MOF membrane strategies for selective lithium extraction from salt lake brine. Advanced Membranes. 5 (2025) 100156.
- [48] J. Li, K. Tuo, C. Fan, G. Liu, S. Pu, Z. Li. Hierarchical Porous Amidoximated Metal-Organic Framework for Highly Efficient Uranium Extraction. Small. 20 (2024) 2306545.
- [49] M.K. Albolkany, C. Liu, Y. Wang, C.H. Chen, C. Zhu, X. Chen, B. Liu. Molecular Surgery at Microporous MOF for Mesopore Generation and Renovation. Angew. Chem. Int. Ed. 60 (2021) 14601-14608.
- [50] D. Li, M. Ye, C. Ma, N. Li, Z. Gu, Z. Qiao. Preparation of a self-supported zeolite glass composite membrane for CO₂ /CH₄ separation. Smart Molecules. 2 (2024) e20240009.
- [51] T. Xia, Y. Wu, T. Ji, W. Hu, K. Yu, X. He, B.H. Yin, Y. Liu. Mixed-matrix membranes incorporating hierarchical ZIF-8 towards enhanced CO₂/N₂ separation. Smart Molecules (2025)

- e20240066.
- [52] Wenjie SHI, Fan LU, Mengwei CHEN, Jin WANG, Y. HAN. Synthesis and host-guest properties of imidazolium-functionalized zirconium metal-organic cage. Chin. J. Inorg. Chem. 41 (2025) 105-113.
- [53] Bin HE, Hao ZHANG, Lin XU, Yanghe LIU, Feifan LANG, P. Jiandong. Recent progress in multicomponent zirconium-based metal-organic frameworks. Chin. J. Inorg. Chem. 40 (2024) 2041-2062.
- [54] W. Dong, J. Yan, T. Ji, M. Wu, K. Yu, Y. Liu, W. Hu, Y. Liu. Eliminating lattice defects in UiO-66-NH2 membrane towards high-precision desalination. Adv.Membr. 5 (2025) 100142.
- [55] S. Wang, J.S. Lee, M. Wahiduzzaman, J. Park, M. Muschi, C. Martineau-Corcos, A. Tissot, K.H. Cho, J. Marrot, W. Shepard, G. Maurin, J. Chang, C. Serre. A robust large-pore zirconium carboxylate metal—organic framework for energy-efficient water-sorption-driven refrigeration. Nat. Energy 3 (2018) 985-993.
- [56] B. Li, F.F. Lu, X.W. Gu, K. Shao, E. Wu, G. Qian. Immobilization of Lewis Basic Nitrogen Sites into a Chemically Stable Metal-Organic Framework for Benchmark Water-Sorption-Driven Heat Allocations. Adv. Sci. 9 (2022) e2105556.
- [57] A. Schaate, P. Roy, T. Preusse, S.J. Lohmeier, A. Godt, P. Behrens. Porous Interpenetrated Zirconium-Organic Frameworks (PIZOFs): A Chemically Versatile Family of Metal-Organic Frameworks. Chem.-Eur. J. 17 (2011) 9320-9325.
- [58] G. Wißmann, A. Schaate, S. Lilienthal, I. Bremer, A.M. Schneider, P. Behrens. Modulated synthesis of Zr-fumarate MOF. Micropor. Mesopor. Mat. 152 (2012) 64-70.
- [59] V. Bon, V. Senkovskyy, I. Senkovska, S. Kaskel. Zr(IV) and Hf(IV) based metal-organic frameworks with reo-topology. Chem. Commun. 48 (2012) 8407-8409.
- [60] Y. Bai, Y. Dou, L.H. Xie, W. Rutledge, J.R. Li, H.C. Zhou. Zr-based metal-organic frameworks: design, synthesis, structure, and applications. Chem. Soc. Rev. 45 (2016) 2327-2367.
- [61] S. Wang, H. Ly, M. Wahiduzzaman, C. Simms, I. Dovgaliuk, A. Tissot, G. Maurin, T.N. Parac-Vogt, C. Serre. A zirconium metal-organic framework with SOC topological net for catalytic peptide bond hydrolysis. Nat. Commun. 13 (2022) 1284.
- [62] Y. Sun, C. Song, X. Guo, Y. Liu. Concurrent Manipulation of Out-of-Plane and Regional

- In-Plane Orientations of NH₂-UiO-66 Membranes with Significantly Reduced Anisotropic Grain Boundary and Superior H₂/CO₂ Separation Performance. ACS Appl. Mater. Interfaces. 12 (2020) 4494-4500.
- [63] S. Chen, M. Wahiduzzaman, T. Ji, Y. Liu, Y. Li, C. Wang, Y. Sun, G. He, G. Maurin, S. Wang, Y. Liu. Oriented Titanium-MOF Membrane for Hydrogen Purification. Angew. Chem. Int. Ed. 64 (2025) e202413701.
- [64] P.S. Gauna, A.A.G. Blanco, D. Barrera, J. Villarroel-Rocha, J.P. Hinestroza, M. Kimura, M.L. Kim, E.H. Otal, K. Sapag. Influence of defect engineering on the hydrogen and methane adsorption capacity in HKUST-1 like structure MOF. Adsorption. 29 (2023) 351-361.
- [65] J. Van Aelst, M. Haouas, E. Gobechiya, K. Houthoofd, A. Philippaerts, S.P. Sree, C.E.A. Kirschhock, P. Jacobs, J.A. Martens, B.F. Sels, F. Taulelle. Hierarchization of USY Zeolite by NH4 OH. A Postsynthetic Process Investigated by NMR and XRD. J. Phys. Chem. C. 118 (2014) 22573-22582.
- [66] X. Wang, L. Zhai, Y. Wang, R. Li, X. Gu, Y. Yuan, Y. Qian, Z. Hu, D. Zhao. Improving Water-Treatment Performance of Zirconium Metal-Organic Framework Membranes by Post-Synthetic Defect Healing. ACS Appl. Mater. Interfaces. 9 (2017) 37848-37855.
- [67] K.H. Lasisi, X. Wu, K. Zhang, R.W. Field. Acid-stable nanofiltration membranes: Emerging materials for sustainable separation in harsh and extreme conditions. Adv. Membr. 5 (2025) 100169.
- [68] X. Liu, N.K. Demir, Z. Wu, K. Li. Highly Water-Stable Zirconium Metal-Organic Framework UiO-66 Membranes Supported on Alumina Hollow Fibers for Desalination. J. Am. Chem. Soc. 137 (2015) 6999-7002.
- [69] Z. Wang, L. Huang, X. Dong, T. Wu, Q. Qing, J. Chen, Y. Lu, C. Xu. Ion sieving in graphene oxide membrane enables efficient actinides/lanthanides separation. Nat. Commun. 14 (2023) 261.
- [70] Y. Yao, J. Liao, X. Xu, C. Huang, M. Fu, K. Chen, L. Ma, J. Han, L. Xu, H. Ma. Hydrazide and amidoxime dual functional membranes for uranium extraction from seawater. J. Mater. Chem. A. 12 (2024) 1528-1538.
- [71] M. Hao, Y. Xie, X. Liu, Z. Chen, H. Yang, G. Waterhouse, S. Ma, X. Wang. Modulating Uranium Extraction Performance of Multivariate Covalent Organic Frameworks through

- Donor-Acceptor Linkers and Amidoxime Nanotraps. JACS Au. 3 (2023) 239-251.
- [72] Z. Yuan, X. Zhu, M. Li, W. Lu, X. Li, H. Zhang. A Highly Ion-Selective Zeolite Flake Layer on Porous Membranes for Flow Battery Applications. Angew. Chem. Int. Ed. 55 (2016) 3058-3062.
- [73] N. Zhang, B. Yang, J. Huo, W. Qi, X. Zhang, X. Ruan, J. Bao, G. He. Hydration structures of vanadium/oxovanadium cations in the presence of sulfuric acid: A molecular dynamics simulation study. Chem. Eng. Sci. 195 (2019) 683-692.
- [74] J. Zhou, Y. Liu, P. Zuo, Y. Li, Y. Dong, L. Wu, Z. Yang, T. Xu. Highly conductive and vanadium sieving Microporous Tröger's Base Membranes for vanadium redox flow battery. J. Membr. Sci. 620 (2021) 118832.
- [75] S. Kim, J. Choi, C. Choi, J. Heo, D.W. Kim, J.Y. Lee, Y.T. Hong, H. Jung, H. Kim. Pore-Size-Tuned Graphene Oxide Frameworks as Ion-Selective and Protective Layers on Hydrocarbon Membranes for Vanadium Redox-Flow Batteries. Nano Lett. 18 (2018) 3962-3968.
- [76] J. Wang, S. Zhuang. Extraction and adsorption of U(VI) from aqueous solution using affinity ligand-based technologies: an overview. Rev. Environ. Sci. Bio-Technol. 18 (2019) 437-452.
- [77] B. Li, Q. Sun, Y. Zhang, C.W. Abney, B. Aguila, W. Lin, S. Ma. Functionalized Porous Aromatic Framework for Efficient Uranium Adsorption from Aqueous Solutions. ACS Appl. Mater. Interfaces. 9 (2017) 12511-12517.
- [78] J. Borden, J. Gilron, D. Hasson. Analysis of RO flux decline due to membrane surface blockage. Desalination. 66 (1987) 257-269.
- [79] Y.H. Choi, J.H. Kweon, D.I. Kim, S. Lee. Evaluation of various pretreatment for particle and inorganic fouling control on performance of SWRO. Desalination. 247 (2009) 137-147.
- [80] D. Guan, Z. Hu, P. Xie, Z. Sun, Z. Zhang, Y. Shan, C. Gong, Y. Wu. Osmotic cleaning to control inorganic fouling of nanofiltration membrane for seawater desalination. J. Environ. Chem. Eng. 11 (2023) 110551.
- [81] W. Daxin, S. Meng, W. Xiaolin. How to evaluate concentration polarization in the process of liquid membrane separation. Membr. Sci. Tech. 25 (2005) 64-68, 79.

Highlights

- Well-intergrown MIP-201 membrane was first prepared through epitaxial growth.
- Both MIP-201 powders and membranes exhibited excellent water and chemical stability.
- The UO₂²⁺ rejection rate (98.5%) of MIP-201 membrane was much higher than other smaller-sized metal ions (2-7%).
- The ideal Fe³⁺/UO₂²⁺ selectivity of MIP-201 membrane was the highest in comparison with the literature.

Declaration of interests

☑ The authors declare that they have no known competing financial interests or personal relationships hat could have appeared to influence the work reported in this paper.
□The authors declare the following financial interests/personal relationships which may be considered as potential competing interests: